A prediction model of death probability for guiding wireless recharging in sensor networks

Ping Zhong, Aikun Xu, Shu Lin and Xiaoyan Kui*

School of Computer Science and Engineering,
Central South University,
Changsha, 410073, China
Email: ping.zhong@csu.edu.cn
Email: aikunxu@csu.edu.cn
Email: ludwiglin@163.com
Email: xykui@csu.edu.cn
*Corresponding author

Abstract: Wireless power transmission (WPT) technology is usually used to maintain the continuous operation of sensor nodes. However, when large amounts of data need to be processed, the node may enter an abnormal death state because it cannot be charged in time. Therefore, a prediction of node death probability is crucial to guide the charging path planning for charging vehicles. In this paper, we build an analysis model based on a Markov fluid queue (MFQ) model with the aim of creating harvest-store-use (HSU) and harvest-then-use (HTU) models of the node. Specifically, the proposed models involve a Markov process, a queuing model, and a successive fluid process. The result shows that the abnormal death probability calculated by the model is approximately 0.1% different from the probability of death obtained by simulation. Meanwhile, by comparing the two modes of energy usage, we find that HTU is better than HSU.

Keywords: abnormal death; MFQ; Markov fluid queue; WSN; wireless sensor network; WRSN; wireless rechargeable sensor network; WPT; wireless power transmission; WET; wireless energy transmission.

Reference to this paper should be made as follows: Zhong, P., Xu, A., Lin, S. and Kui, X. (2021) 'A prediction model of death probability for guiding wireless recharging in sensor networks', *Int. J. Sensor Networks*, Vol. 37, No. 2, pp.125–139.

Biographical notes: Ping Zhong received her PhD in Communication Engineering from Xiamen University, China, in 2011. She is currently an Associate Professor with the School of Computer Science and Engineering at Central South University. Her research interests include machine learning, data mining, and networks protocol design. She is a member of ACM, CCF, IEICE and IEEE.

Aikun Xu is currently a Master student in the School of Computer Science and Engineering, Central South University, Changsha, China. He received his BS in the School of Computer Science from South Central University for Nationalities, Wuhan, China, in 2019. His research interests include machine learning, scheduling, electric vehicles, and wireless networks.

Shu Lin is currently an undergraduate student in the School of Computer Science and Engineering, Central South University, Changsha, China. His research interests include machine learning, scheduling, electric vehicles, and wireless networks.

Xiaoyan Kui received her PhD in Computer Science from Central South University, China, in 2012. She is currently a Professor with the Department of Computer Science and Technology at Central South University. Her research interests include wireless sensor network, vehicular network, and information visualisation.

This paper is a revised and expanded version of a paper entitled 'Markov fluid queue model for rechargeable sensor nodes with abnormal death' presented at *2017 IEEE International Symposium on Parallel and Distributed Processing with Applications and 2017 IEEE International Conference on Ubiquitous Computing and Communications (ISPA/IUCC)*, Guangzhou, China, 12–15 December, 2017.

1 Introduction

In modern society, there are plenty of applications based on networked low-cost nodes that are distributed in space, such as in wireless sensor networks (WSNs) (Masotti et al., 2016). Wireless sensor networks are commonly used for environmental monitoring (Gao et al., 2017; Mukherjee et al., 2017; Liu et al., 2018). The sensor nodes are battery-powered, but their energy is limited (Liu et al., 2018; Tang et al., 2018; Jan et al., 2017). For low-power sensor nodes, careful power management and power conservation are critical to device lifetime and effectiveness (Deng et al., 2016). Replacing batteries is infeasible due to the large quantity of nodes (Correia et al., 2017). A wireless rechargeable sensor network (WRSN) can increase the overall lifetime of the network by charging remotely (Zhong et al., 2018; Guimarães et al., 2020). Energy harvesting (EH) from the environment, such as from solar (Zhou et al., 2019), wind (Sah and Amgoth, 2020) and ambient radio frequency (RF) waves (Zhang et al., 2019), is an effective way to solve replacing batteries. However, the acquisition of energy from the environment is failing to provide sustained and stable energy.

Wireless power transmission (WPT)/wireless energy transmission (WET) technology is a wireless charging technology, transmits electromagnetic energy without interconnecting cords (Lu et al., 2015). WPT/WET is a potential solution to solve the power source uncertainty in EH. However, sometimes, the power source cannot reach the nodes that need charging in time, which may lead to the abnormal death of sensor node (Lin et al., 2016; Tomar et al., 2016). Abnormal death is different from that of temporal death (Tan et al., 2016; Kaur et al., 2019). An abnormal death may occur when transmitting large amounts of data and the nodes cannot replenish their energy in time, while temporal death means that the nodes were unable to collect enough energy. Death probability is defined as the probability of abnormal death in this paper.

The residual energy of the node is higher than a threshold (the minimum energy value to maintain normal operation), the node is guaranteed to work properly. However, when the power source cannot provide timely energy charging for the nodes, the exhausted nodes will enter the inactive state and be unable to send or receive data, which is referred to as the abnormal death state. To address this problem, this paper presents a model and an analysis of a WRSN with abnormal death using the Markov fluid queue (MFQ) model. The main contributions of this paper are as follows.

- There is no corresponding mathematical model to predict the abnormal death probability of nodes in a WRSN using WET as an energy supplement. To further understand the relationship among the residual energy, charging process and working mechanism, we use a Markov process to simulate the node charging process, a queuing model to describe the normal working mechanism of the nodes, and a successive fluid process, instead of a discrete model, to determine the node residual energy level in WRSNs, which makes the model more precise. The model we established is a comprehensive analytical framework that characterises WRSNs with abnormal death. Furthermore, we combine the queuing analytical model with the IEEE 802.11b protocol to obtain the transmission probabilities of nodes at any time slot, which will improve the model's accuracy. As far as we know, this is the first time that sensor nodes in a WRSN have been modelled using WET as an energy supplement. This model can play a guiding role in charging planning under a network scenario.
- At present, most of the studies on modelling in a WRSN consider nodes having a harvest-store-use (HSU) structure as the charging process, where the working process of the nodes is performed in series. To generalise our model to real-world applications, we also model nodes with a harvest-then-use (HTU) structure as the charging process, where it acts in parallel with the nodes' working process. Additionally, we compare the performance of the two working nodes and find that the performance of HTU is better than that of HSU. Thus, the model is suitable for predicting node abnormal death under multimode operation, and it can also ensure the applicability of a multienvironment, making the research more meaningful.
- Through a theoretical analysis and simulation study, we verify the accuracy of the model based on the network simulation tool NS-3. The experiment has shown that the abnormal death probability calculated by the model is approximately 0.1% different from the probability of death obtained by simulation, which demonstrates the outstanding accuracy of the model.

The structure of the rest of the paper is organised as follows. The related works are introduced in Section 2. In Section 3, the system model and the assumption of nodes with the abnormal death state are given. The steady state density analysis is shown in Section 4. The numerical results that the node can perform under different working modes is given to illustrate the theoretical findings in Section 5. Finally, Section 6 concludes the work.

2 Related work

This section divide the existing research into two parts. One part seeks the best data transmission and resource allocation strategies for meeting different objectives and network scenes, and the other part models the energy consumption and the lifetime of the node.

For the former, we summarise the relevant research as follows. In Singh et al. (2020), the energy consumption and energy protection strategies in WSNs were summarised. In Sudevalayam et al. (2010) and Sah et al. (2020), the structure of EH sensor nodes and the energy storage method were mainly discussed. Both Biason et al. (2014) and Biason and Zorzi (2015) presented a two-dimensional discrete time stochastic process to describe the time slot system in WSN to maximise the steady-state average data transmission rate. In Chan et al.

(2015), considering the residual energy of the node, ambient energy source and the QoS requirement, a Markov decision process was built to model the network state of a node to obtain the QoS metrics. The authors in Ryu et al. (2019) set up an energy management mechanism for the ambient energy source to achieve system targets. Shu et al. (2016) proposed a joint energy replenishment and scheduling mechanism for the purpose of maximising the network's lifetime. Wu et al. (2020) studied the issue of combining simultaneous wireless charging with mobile data collection.

For the second aspect, the main findings are summarised as follows. In Naderi et al. (2012), a semi-Markov model was established to estimate the node remaining energy distribution, and a new method of analysis called 'energy transient' was introduced. The authors In Seyedi and Sikdar (2008) modelled the EH sensor nodes and the model could be used to calculate the packet loss rate due to environmental factors. Susu et al. (2008) presented a discrete time Markov chain model called 'DTMC' for EH sensor nodes that could calculate the probability distribution of the expected downtime. The authors In Ventura and Chowdhury (2011) established a model focused on single or multiple energy sources. In Naderi et al. (2015), a 2D and 3D model were established in a WRSN that had multiple RF energy transmitters. Lei et al. (2009) proposed a generic framework to describe the single-hop transmission policy for rechargeable sensor nodes, in which a Markov chain model was established to capture different modes of energy renewal. In Jung et al. (2009), the author developed parametric lifetime models for trigger-driven and duty-cycle driven nodes. Tan et al. (2016) considered the temporal death in WSN and established a model to discuss various performance aspects of an energy harvesting wireless sensor network (EH-WSN). Tunc and Akar (2017) used a finite-state continuous time Markov chain model to describe the energy harvesting process and proposed a risk-theoretic MFQ model for the computation of the first battery outage probabilities in a given finite time horizon. In Table 1, we summarise the related research.

None of the above research considered the special issue for WRSNs, that is, abnormal death, as we discussed above, which plays an important role in the lifetime of sensor networks. There are three main differences between our paper and the works of Tan et al. (2016) and Tunc and Akar (2017). The first point is that the scenes that we consider are different. The second point is that we combine IEEE 802.11b for modelling to make the model analysis closer to reality, which is more accurately embodied in the calculation of the parameters. The third point is that we consider a variety of work modes in the node, which will make the model versatile. In general, based on a MFQ model, we build a model that can effectively predict the node abnormal death probability. Evaluating the node abnormal death in a network makes the model more feasible and convenient for future research, such as in the mobile path optimisation problem for charging vehicles and in the determination of the charging threshold.

3 System model and assumption

This paper consider WRSN nodes with a HSU architecture (Sudevalayam et al., 2010) and nodes with HTU architecture, which has an energy harvesting system and a rechargeable battery that can be powered by the charging vehicle. As shown in Figure 1, there are two optional modes for energy usage in a rechargeable battery (HSU and HTU) in a gridline. In HSU, the node can send and receive data only when energy buffer X is full (size B) after being powered by the charging vehicle. Therefore, the charging process and the data transmission work serially. In HTU, the node can work if the residual energy $X(t)$ is greater than the minimum charging threshold P_{low}, regardless of whether it is charged. That means the charging process and the data transmission can work in parallel. This paper will set up a model based on these two modes.

Figure 1 The energy usage diagrams under the two modes (see online version for colours)

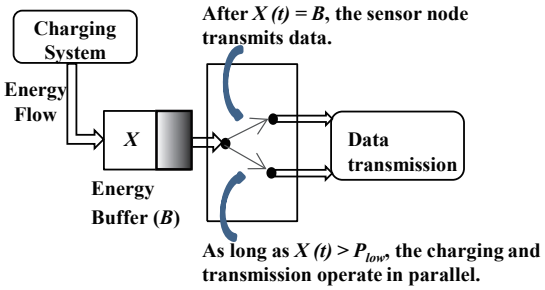

To reduce the energy consumption, we assume that the node uses the combination of duty cycling and beacon intervals (BIs). In this paper, we use the random sleep-awake schedule, which means that each node keeps a sleep-active schedule independent of the others (Tan et al., 2016). As shown in Figure 2, the active stage includes a fixed period of listening and BIs. An Announcement Traffic Indication Message (ATIM) window and a data window make up each BI. The node is allowed to send data only when it can successfully transmit an ATIM frame in the ATIM window. Additionally, a node that neither transmits nor receives an ATIM frame in the ATIM window goes into sleep mode in the data window to save energy and to wait for the next BI (Swain et al., 2014). Zheng et al. (2004) has proven that a data window is enough to successfully transmit a data frame after the successful transmission of an ATIM frame. Therefore, we also assume that a data window is sufficient to transmit a data frame.

Figure 2 Illustration of the combination of BI and duty cycling (see online version for colours)

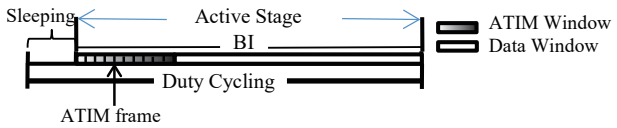

3.1 Semi-Markov chain overview

We use a semi-Markov chain to model the working process of sensor nodes, which include listening (L), transmitting (T),

Table 1 Related works in modelling

Literature	*Scene*	*Energy supply*	*Model kernel*	*Abnormal death*	*Objective*
Naderi et al. (2012)	WSN	EH	Stochastic semi-Markov model	No	To deduce the distribution of node remaining energy
Seyedi and Sikdar (2008)	WSN	EH	Markov chain model	No	To calculate the probability of packet loss due to environmental factor
Susu et al. (2008)	WSN	EH	Markov chain model	No	To consider the uncertainty of the power source by developing a model that maximises the lifetime of the system
Ventura and Chowdhury (2011)	Body sensor networks (BSNs)	EH	Markov model	No	To predict future consumption and residual availability of energy in a sensor node
Naderi et al. (2015)	WSN	WET	Base on communication principle	No	To study the closed matrix forms of harvestable power at any given point in 2D and 3D space considering constructive and destructive interference
Lei et al. (2009)	WSN	EH	Markov chain model	No	To describe different modes of energy renewal and derive an optimal transmission policy for sensors with different energy budgets
Jung et al. (2009)	WSN	WET	Semi- Markov model	No	To develop a lifetime models for trigger-driven and duty-cycledriven nodes
Tunc and Akar (2017)	WSN	EH	Risk- theoretic Markov fluid queue model	Yes	To compute the first battery outage probabilities in a given finite time horizon
Tang and Tan (2016)	WSN	EH	Markov fluid queue model	Yes	To discuss various performance aspects of the EH-WSN node with temporal death
Our paper	WRSN	WET	Markov fluid queue model	Yes	To predict the probability of node death and steady energy consumption

sleeping (S), charging (C), and abnormal death (D). The state transition diagrams of HSU and HTU nodes are respectively shown in Figure 3. The solid line represents the transitions between the working states, while the dashed line indicates that the node will return to the sleeping state if the energy level satisfies the minimum condition for the node to send data in different modes. In both HSU and HTU, the working state of the nodes is unchanged, and the following assumptions are satisfied.

3.1.1 Sleeping state

The node either remains in a sleeping state or experiences abnormal death with a probability of P_{SD}, or it is in a charging state with a probability of P_{SE} if the node is in the sleeping state. After experiencing the sleeping state for a fixed sleeping period T_S, the node switches to the listening state with a probability P_{SL}. We consider the existence of two charging thresholds, namely, the upper threshold P_{high} and the lower threshold P_{low}. When the residual energy reaches P_{high}, the node needs charging, and the node reaching the upper threshold cannot work normally for a long time. When the residual energy of the node reaches the lower threshold and cannot be charged in time, the node will fall into a state of abnormal death. When the residual energy of the nodes is in the interval [0, P_{high}], it will obey a uniform distribution. Therefore, the probability of falling into an abnormal death is $P_{SD} = P_{low}/P_{high}$, where $P_{low} = P_{high} - J \times d_s/v$, and P_{high} is the minimum energy required for all of the data frames to be transmitted. Here, we assume that the farthest distance between contiguous nodes is J, the energy consumption rate in the sleeping state is d_s, and the moving speed of the vehicle is v.

Figure 3 Semi-Markov chain of the rechargeable sensor node in different modes

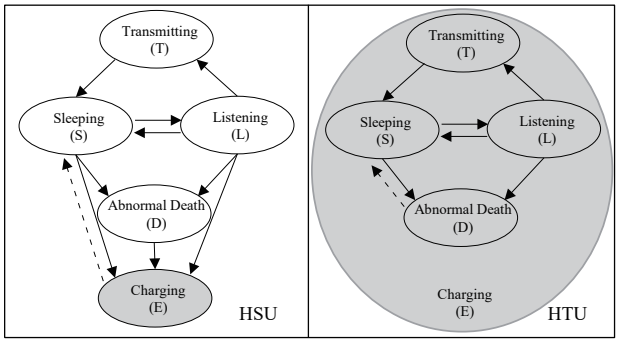

3.1.2 Listening state

The listening state occurs in the ATIM window. If an ATIM frame is successfully received or sent, the corresponding node will enter the data window and wait for the data transmission. After the data frames in the data buffer have been processed and the node reenters the sleeping state, the corresponding probability is P_{LS}. Otherwise, if there is no receiving or sending of ATIM frames, the node will enter into the sleeping state directly after the end of the ATIM window. During the active period, it is reasonable to assume that the data frame arrival rate obeys a Poisson distribution with an average rate of λ. Therefore, the probability of changing from the listening

state to the sleeping state is $P_{LS} = e^{-\lambda T_w}$, where T_w is the wakeup stage. The charging probability in the listening state is the same as the one in the sleeping state. As a result, $P_{LD} = 1 - P_{LS} - P_{LE} - \tau$ is the probability of changing from the listening state to the abnormal death state, in which τ is the probability of sending a data frame in any time slot of the data window.

3.1.3 Transmitting state

For simplicity, we assume that an ATIM frame has three retransmissions. After successfully transmitting an ATIM frame, the node will send a data frame. Otherwise, the node waits for the next ATIM window to continue. When the data frame is not successfully transmitted, the retransmission will be repeated until the maximum retransmission time M is reached, at which time the corresponding data frame is discarded. For each transmission, it is reasonable to assume that the transmission time of data frames follows the exponential distribution of mean T_{tr}. The node enters the sleeping state when all of the data frames in the data buffer pool are processed.

3.1.4 Abnormal death

In our model, as soon as the remaining energy reaches P_{low} and cannot be charged in time, the node enters into the state of abnormal death and becomes inactive, resulting in a loss of perception and communication. The node must stay in the abnormal death state until it is charged by the wireless charging vehicle. Although the operation of the node is different in HSU and HTU, in both cases, the node will wake up and return to the sleeping state and resume normal operation.

3.2 Modelling the normal working process

We assume that the size of each packet is fixed and that, when the packet arrives, it will cache in the data buffer pool and wait for processing. The symbol K represents the maximum number of frames that can be stored in the data buffer pool. We use $\{A\} = \{A(k,m), 1 \le k \le K, 1 \le m \le M\}$ to describe the transmission process of the nodes. In this process, a retransmission is described as $A(k,m)$, in which k represents the data frame in the data buffer pool, and m is the number of retransmissions. We depict the relationship between the data frame transmitted and the number of retransmissions in detail in Figure 4. In particular, the transition from $A(k,m)$ to $A(k,m+1)$ means that the k data frame is not successfully transmitted with the probability p_f in m retransmissions. Additionally, the transition from $A(k,M)$ to $A(k+1,1)$ means that the current frame has been transmitted M times, and it cannot be retransmitted again. Whether in HSU or HTU, the state transitions of the transmitting nodes are the same.

We use the random process $\varphi_T = \{\varphi_T(t), t \ge 0\}$ to represent the working mechanism of the node. The node works normally as described above if the node does not fall into a state of abnormal death. In contrast to the semi-Markov chain, the continuous time Markov chain (CTMC) is a special semi-Markov chain. We can regard φ_T as a CTMC, where the state space is $\Omega_T = \{S, L, T\} = \{S, L, A(A,m), 1 \le k \le K, 1 \le m \le M\}$, and the infinitesimal generator of Ω_T is $\mathbf{Q}_T = ([\mathbf{Q}_T]_{ij})$. As listed in Table 2, we can obtain $\mathbf{Q}_T$ according to the node state conversion diagram and semi-Markov chain when $i \ne j$, and we can also obtain $[\mathbf{Q}_T]_{ii} = -\sum_{i \ne j}[\mathbf{Q}_T]_{ij}$ when $i = j$.

Figure 4 The detailed state transition diagram of transmitting the state of a sensor node (see online version for colours)

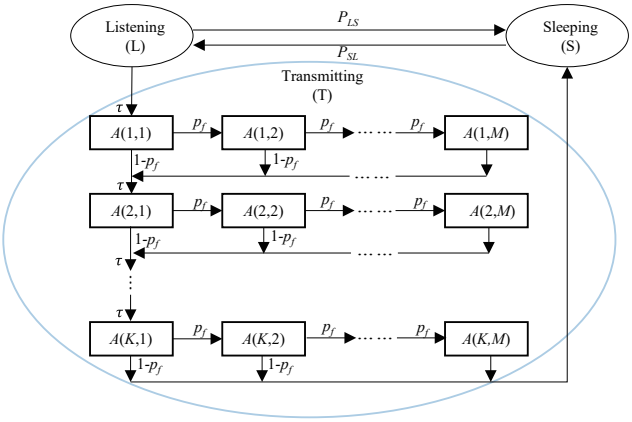

Table 2 The calculation of the state transition

From	*To*	*Rate*	*Note*
S	L	P_{SL}	
L	S	P_{LS}	
L	$A(1,1)$	τ	$j = 1, 2, 3, ..., M-1$
$A(K,M)$	S	1	
$A(i,j)$	$A(i,j+1)$	p_f	$m = 1, 2, 3, ..., K$
$A(i,j)$	$A(i+1,1)$	$(1-p_f)\tau$	
$A(m,M)$	$A(m+1,1)$	τ	$i = 1, 2, 3, ..., K-1$
other	other	0	

3.3 Modelling of the node charging process

The node sends a charging request when the residual energy is less than P_{high}. The wireless charging vehicle charges the node until the node's power is full (size *B*). When the node is in HSU, each time it is charged to *B*, the node enters the sleeping state and then switches to the listening state after a fixed time T_S. In HTU, once the node is powered up to P_{low}, it returns to the sleeping state and continues to work normally.

We define $d_{\varphi_T(t)}$ as the energy consumption rate at time t, and d_E, d_T, d_L, d_S respectively represent the corresponding energy consumption rates in the state E, T, L and S. For convenience, we assume that the energy consumption rate in each state is a fixed value. In addition, to ensure the normal operation of the node, we consider the energy of the node supplementation as greater than the energy consumed by the transmission state. Accordingly, we reasonably assume that $d_E > d_T > d_L > d_S$ and that, when the node is in a state of abnormal death, it neither receives nor sends data frames, so it does not consume energy.

The current research usually builds the energy harvesting activity into a two-state Markov model. In Ho et al. (2010)

and (Zhang, 2013), the accuracy of using a two-state Markov model to describe the energy harvesting process is proven. The charging behaviour is also a special energy harvesting activity. Therefore, we continue to follow this approach, and we build the node charging process as a two-state Markov model $\varphi_E = \{\varphi_E(t), t \neq 0\}$, where the state space Ω_E has two kinds of states $\{E, N\}$, and E represents the charging state and N represents the noncharging state.

Therefore, we can get the infinitesimal generator $\mathbf{Q}_E$ of φ_E according to (1). The symbol ρ_E (or ρ_N) represents the conversion probability from the E (or N) state to the N (or E) state.

$$\mathbf{Q}_E = \begin{bmatrix} -\rho_N & \rho_N \\ \rho_E & -\rho_E \end{bmatrix} \tag{1}$$

3.4 Detailed model description

In order to predict the death probability of a node, we design a MFQ model to solve the discrete change of the node state and the continuous change of the node energy simultaneously, i.e., calculating the net charging rate and remaining of the node. Then, the MFQ model is divided into three situations: the residual energy the rechargeable sensor nodes is greater than or equal to the upper charging threshold (i.e., $X(t) \geq P_{high}$), the residual energy the rechargeable sensor nodes is greater than the lower charging threshold and less than the upper charging threshold (i.e., $P_{low} < X(t) < P_{high}$), and the residual energy the rechargeable sensor nodes is less than or equal to the lower threshold (i.e., $X(t) \leq P_{low}$). Finally, the loop of the node state is realised by judging the residual energy of the current rechargeable sensor nodes. The detailed description of the model is as follows.

Previous research has usually modelled the energy change process of nodes as a discrete Markov chain. Discrete Markov chains are a simple but powerful approach for solving the steady state probability of a system. In Tang and Tan (2016), discrete state models are applied when the considered system behaviour can be represented as a finite or countable set. We note that the hybrid framework model (discrete and continuous) is more versatile in its performance analysis. In our considered scenario, the change of the node state is discrete, and the corresponding residual energy change is continuous; moreover, the energy varies with the state of the node. Therefore, we consider a hybrid framework model, the MFQ model, to describe normal working process and charging process of a node.

The MFQ model is a two-dimensional Markov process where the first dimension (level) changes linearly with the second dimension (stage) (Da Silva Soares and Latouche, 2009). The stage is a time-dependent evolution of the Markov process in a finite space. By definition, we combine a node's normal working process φ_T with its charging process φ_E to form the process φ as $\varphi(t) = \{\varphi_E(t), \varphi_T(t), t \geq 0\}$. In Tan et al. (2016), if the remaining energy of the node is not zero, the infinitesimal generator of φ in the corresponding state space $\Omega = \Omega_E \times \Omega_T$ is $\mathbf{Q} = \mathbf{Q}_E \oplus \mathbf{Q}_T$, where $\oplus$ is the Kronecker sum. Similarly, we can also define $\Omega = \Omega_{EE} \cup \Omega_{EN}$ according to the node's charging state, where Ω_{EE} is the charging state space in the node's state change process φ, while Ω_{EN} is the noncharging state space for the same process. The state change process φ varies for different working modes. Tables 3 and 4 list the net charging rate under different state spaces.

In HSU, the net charge rate r_i for the noncharging state is different from that of the charging state. The backslash indicates that the state that does not exist. Specially, the net charge rate in different states at time t can be obtained by equation (2).

$$r_i = \begin{cases} d_E & \text{i=1} \\ -d_{\varphi_T(t)} & \text{i=2,3,4,...,3+}KM \end{cases} \tag{2}$$

When $i = 1$, the node is in the charging state without any other energy consumption. Nevertheless, the net charge rate is equal to the negative energy consumption in different normal working states when $i \neq 1$. Similarly, we can obtain the net charge rate r_i in different states in HTU as (3).

$$r_i = \begin{cases} d_E - d_{\varphi_T(t)} & \text{i=1,2,3,...,2+}KM \\ -d_{\varphi_T(t)} & \text{i=3+}KM\text{, 4+}KM\text{,...,4+2}KM \end{cases} \tag{3}$$

When the node is in Ω_{EE}, both the charging rate and the energy consumption of each state should be considered. The concept of the net charging rate is based on the simultaneous consideration of the node charging rate and the energy consumption rate, which can be considered as the net fluid rate in the MFQ model. In the charging state, the net charge rate matrix is $\mathbf{R}_E = diag(r_i, i \in \Omega_{EE})$. Similarly, we obtain $\mathbf{R}_N = diag(r_i, i \in \Omega_{EN})$ and $\mathbf{R} = diag(\mathbf{R}_E, \mathbf{R}_N)$ (Tang and Tan, 2016). At the same time, the energy consumption matrix in state space Ω can be defined as $\mathbf{R}_d = diag(d_k, k \in \Omega)$.

We use $X = \{X(t), 0 \leq X(t) \leq B, t \geq 0\}$ to describe the residual energy change of the rechargeable sensor nodes; the evolution of X can be expressed by the following equation.

$$\frac{dX(t)}{dt} = \begin{cases} d_E & X(t) = 0 \\ r_i & 0 < X(t) < B \\ 0 & X(t) = B \end{cases} \tag{4}$$

The final MFQ model $\{X, \varphi\}$ can be obtained based on the above modelling of a node's working process and charging process. In the MFQ model, X describes the change process of the fluid level that corresponds to the residual energy change in the energy buffer, and φ is the phase change, which is related to the working mechanism of the node. On this basis, regardless of the kind of working mode the node is in, we divide the Markov flow queue model into the following three situations in the state space.

- In the case of $X(t) \geq P_{high}$, the infinitesimal generator $\mathbf{Q}$ of the node state variety transversion φ in the state space Ω can be expressed as follows.

$$\mathbf{Q} = \begin{bmatrix} \mathbf{Q}_{EE} & \mathbf{Q}_{EN} \\ \mathbf{Q}_{NE} & \mathbf{Q}_{NN} \end{bmatrix} \tag{5}$$

  In $\mathbf{Q}$, the element of the submatrix $\mathbf{Q}_{EE}$ is $[\mathbf{Q}]_{(a,b)}$ with $a \in \Omega_{EE}$ and $b \in \Omega_{EE}$, which represents the change from a to b, and the other submatrices in $\mathbf{Q}$ have similar meanings. $\mathbf{Q}_{NE}$ (or $\mathbf{Q}_{EN}$) represents the change from the N (or E) state to the E (or N) state.

Table 3 The net charging rate r_i IN HSU

State	(E,S)	(E,L)	$(E,A(1,1))$	.....	$(E,A(K,M))$	$(E,\backslash)$	
Net charge rate	$\backslash$	$\backslash$	$\backslash$	.....	$\backslash$	r_1	$\mathbf{\Omega}_{EE}$
State	(N,S)	(N,L)	$(N,A(1,1))$	.....	$(N,A(K,M))$		
Net charge rate	r_2	r_3	r_4	.....	$r_{(3+KM)}$		$\mathbf{\Omega}_{EN}$

Table 4 The net charging rate r_i IN HTU

State	(E,S)	(E,L)	$(E,A(1,1))$	.....	$(E,A(K,M))$	
Net charge rate	r_1	r_2	r_3	.....	$r_{(2+KM)}$	$\mathbf{\Omega}_{EE}$
State	(N,S)	(N,L)	$(N,A(1,1))$	.....	$(N,A(K,M))$	
Net charge rate	$r_{(3+KM)}$	$r_{(4+KM)}$	$r_{(5+KM)}$	.....	$r_{(4+2KM)}$	$\mathbf{\Omega}_{EN}$

- In the case of $P_{low} < X(t) < P_{high}$, the node state space is $\Omega_{EE} \cup \Omega_{EN} \cup \{D\}$ because the node is either waiting for charging or in the charging state. Thus, the state transition matrix that contains the probabilities of these transitions on this state space is denoted by $\mathbf{P}$ as follows.

$$\mathbf{P} = \left[\mathbf{P}_{NE}, \mathbf{P}_{NN}, \mathbf{P}_{ND}\right] \tag{6}$$

where $\mathbf{P}$ is a block matrix consisting of $\mathbf{P}_{NE}$, $\mathbf{P}_{NN}$, and $\mathbf{P}_{ND}$ with an appropriate matrix size. The matrix size should depend on the maximum capacity of data buffer (K) and the maximum retransmission times (M). If X does not reach the lower threshold P_{low} and the node is charged in time, we can obtain $\mathbf{P}_{NE}$ through the following charging probability matrix.

$$\mathbf{P}_{NE} = \begin{bmatrix} \mathbf{P}_E & \mathbf{0} \\ \mathbf{0} & \mathbf{0} \end{bmatrix} \tag{7}$$

$$\mathbf{P}_E = \begin{bmatrix} \rho_E & 0 \\ 0 & \rho_E \end{bmatrix} \tag{8}$$

$\mathbf{P}_{NE}$ is a block matrix that represents the conversion from normal working state (noncharging state) to the charging state. The $\mathbf{0}$ in $\mathbf{P}_{NE}$ represents a zero matrix where the matrix size is adapted to the $\mathbf{P}_{NE}$. Based on the charging probability, $\mathbf{P}_E$ can be obtained. If the residual energy X reaches the lower limit threshold and still cannot replenish energy in time, the node will fall into a state of abnormal death. Thus, $\mathbf{P}_{ND}$ and $\mathbf{P}_{NN}$ can be written as follows, where $\mathbf{1}$ is a unit matrix with the same size as $\mathbf{P}$. $\mathbf{P}_{ND}$ represents the conversion from the normal working state (noncharging state) to the abnormal death state. $\mathbf{P}_{NN}$ is $[\mathbf{P}]_{(a,b)}$ with $a \in \{\Omega_{EE} \cup \Omega_{EN} \cup \{D\}\}$ and $b \in \{\Omega_{EE} \cup \Omega_{EN} \cup \{D\}\}$, which represents the change from a to b.

$$\mathbf{P}_{ND} = \begin{bmatrix} P_{SD} & P_{LD} \end{bmatrix} \tag{9}$$

$$\mathbf{P}_{NN} = \mathbf{1} - \mathbf{P}_{NE} - \mathbf{P}_{ND} \tag{10}$$

- In the case of $X(t) \le P_{low}$, a node's state space is $\Omega_{EE} \cup \Omega_{EN} \cup \{D\}$ because the node falls into a state of abnormal death. The state transition rate matrix $\mathbf{T}$ in the state space is expressed as (11). It can be noted that when the fluid level is zero in the model, the node can only be in a state of death. We partition $\mathbf{T}$ according to $\Omega_{EE} \cup \Omega_{EN} \cup \{D\}$ as follows.

$$\mathbf{T} = \left[\mathbf{T}_{DE}, \mathbf{T}_{DN}, \mathbf{T}_{DD}\right] \tag{11}$$

$\mathbf{T}_{DE}$, $\mathbf{T}_{DN}$, and $\mathbf{T}_{DD}$ have similar definitions as $\mathbf{Q}_{EE}$. We can also get the state transition rate through the charging probability ρ_E. $\mathbf{T}_{DE}$ represents the state transition rate from the abnormal death state to the charging state. $\mathbf{T}_{DN}$ represents the state transition rate from the abnormal death state to the normal working state (noncharging state). $\mathbf{T}_{DD}$ is $[\mathbf{T}]_{(a,b)}$ with $a \in \{\Omega_{EE} \cup \Omega_{EN} \cup \{D\}\}$ and $b \in \{\Omega_{EE} \cup \Omega_{EN} \cup \{D\}\}$, which represents the change from a to b.

$$\mathbf{T}_{DE} = \rho_E, \mathbf{T}_{DN} = \mathbf{0}, \mathbf{T}_{DD} = -\rho_E \tag{12}$$

Once the process φ changes into the state in Ω_{EE}, the working principle of the node will be carried out as described in the first situation $X(t) \ge P_{high}$.

4 Steady state density analysis

The above section described our model, and in this section, we solve the steady state density probabilities. In our model, since the state change is irreducible and finite, it has a steady state probability vector $\boldsymbol{\xi}$, which can be calculated by $\boldsymbol{\xi}\mathbf{Q} = \mathbf{0}$ and $\boldsymbol{\xi}\mathbf{1} = \mathbf{1}$. We denote $\mathbf{1}$ as a unit column vector and $\mathbf{0}$ as a zero matrix or vector with the appropriate size. The mean drift of the fluid queue model that exists is calculated by $\mu = \boldsymbol{\xi}_E\mathbf{R}_E - \boldsymbol{\xi}_N\mathbf{R}_N$ (Da Silva Soares and Latouche, 2009). The mean drift μ can also be seen as the net charge rate for the long term development of the entire network, in which $\boldsymbol{\xi}_E = \{\boldsymbol{\xi}_i, i \in \Omega_{EE}\}$ and $\boldsymbol{\xi}_N = \{\boldsymbol{\xi}_i, i \in \Omega_{EN}\}$. The fluid queue model stops functioning when $\mu = 0$. There exists transient variation when $\mu > 0$, and, in this case, we cannot get the steady state densities for every state. When and only when $\mu < 0$, the steady state distribution exists in the fluid queue model (Da Silva Soares and Latouche, 2006). In this paper, considering the appearance of abnormal death, we assume that $\mu < 0$ as the energy charged by the nodes is less than the energy consumed by the nodes in the long run.

We need to calculate the steady state probabilities at all levels of energy. In Tang and Tan (2016), there exists probability masses when the residual energy is zero or full with the corresponding states of abnormal death (D), $(E, \backslash)$ (in HSU), or (E, S) (in HTU). Therefore, the marginal probability density can be defined as follows.

$$\eta_D(0) = \lim_{t\to\infty} P(X(t) = 0, \varphi(t) = D) \tag{13}$$

$$\eta_i(0) = \lim_{t\to\infty} P(X(t) = B, i \in \varphi(t)) \tag{14}$$

For $j \in \Omega$ and $0 < X(t) < B$, the joint distribution of the residual energy and the corresponding probability density function are as follows.

$$F_j(x,t) = P(X(t) \le x, \varphi(t) = j) \tag{15}$$

$$f_j(x,t) = \frac{\partial F_j(x,t)}{\partial x} \qquad 0 < x < B \tag{16}$$

In conclusion, the steady state density vector can be expressed as $\boldsymbol{\pi}(x) = (\pi_j(x), j \in \Omega)$ and $\pi_j(x) = \lim_{t\to\infty} f_j(x,t)$. In addition, we denote $\boldsymbol{\pi}(b+) = \lim_{x\to b+} \boldsymbol{\pi}(x)$ and $\boldsymbol{\pi}(b-) = \lim_{x\to b-} \boldsymbol{\pi}(x)$, which can also be applied to $\boldsymbol{\pi}(0+)$ and $\boldsymbol{\pi}(0-)$. Thus, we obtain the following.

$$\eta_D(0) = (0, \eta_N(0)) \tag{17}$$

$$\eta_i(B) = (\eta_E(B), 0) \tag{18}$$

For $i, j \in \Omega$, $0 < x < B$ and $0 < y < B$, the meaning of $N_{ij}(x,y)$ is the expected number of crossings of level y in phase j, starting from (x,i) and before the first visit either to level 0 or to level B (Da Silva Soares and Latouche, 2006). Based on the initial states $i \in \Omega_{EE}$ and $i \in \Omega_{EN}$, $N_{ij}(x,y)$ can be divided into two parts: $N_E(x,y)$ and $N_N(x,y)$. Their dimensions are $|\Omega_{EE}| \times |\Omega|$ and $|\Omega_{EN}| \times |\Omega|$, respectively. $N_N(o,y) = 0$ because, if the state starts from $(0,i), i \in \Omega_{EN}$, the fluid level remains at zero. Similarly, we can obtain $N_E(B,y) = 0$.

The starting point of this paper is the combination of the charging process and normal working process of a node; for convenience, we assume that it starts from $X(0) = P_{high}$ and that the state at time t is $(X(t), k)$ with $0 < X(t) < B$. We consider the following three state changes at time t.

- The state at time $t - \varepsilon$ that ε tends to 0_+ is $(P_{low}, i), i \in \Omega_{EN}$. Before arriving at time t, there exists a phase transition from (P_{low}, i) to (P_{low}, j), where $j \in \Omega_{EE}$ and where the state changes from (P_{low}, j) to $(X(t), k)$ during the period ε, in which the process of changing from (P_{low}, i) to (P_{low}, j) is a transient variation; as a result, the energy level does not vary with state. The corresponding expression is as follows.

$$A = \int_0^t \sum_{i\in\boldsymbol{\Omega}_{EN}, j\in\boldsymbol{\Omega}_{EE}} \mathbf{F}_i(P_{low}, t-\varepsilon) \mathbf{R}_N(\mathbf{Q}_{NE})_i j \times \mathbf{N}_{jk}(P_{low}, X(t); \varepsilon) d\varepsilon \tag{19}$$

- The state at time $t - \varepsilon$ where ε tends to 0_+ is $(B, i), i \in \Omega_{EE}$. Before arriving at time t, there exists a phase transition from (B, i) to (B, j), where $j \in \Omega_{EN}$ and where the state changes from (B, j) to $(X(t), k)$ during the period ε. The process of changing from (B, i) to (B, j) is a transient variation. Thus, the energy level does not vary with state, and the corresponding expression is as follows.

$$G = \int_0^t \sum_{i\in\boldsymbol{\Omega}_{EE}, j\in\boldsymbol{\Omega}_{EN}} \widetilde{\mathbf{F}}_i(B, t-\varepsilon) \mathbf{R}_E(\mathbf{Q}_{EN})_{ij} \mathbf{N}_{jk}(B, X(t); \varepsilon) d\varepsilon \tag{20}$$

- In the interval $[0, t)$, the residual energy level of the node changes continuously between P_{low} and B when $\varphi(0) \in \Omega_{EE}$.

$$C = \sum_{i\in\boldsymbol{\Omega}_{EE}} P(\varphi(0) = i) \mathbf{RN}_{ik}(P_{low}, X(t); t) \tag{21}$$

Based on the above statement, we can obtain the expression of the probability density function at time t.

$$f_k(X(t), t) = A + G + C \tag{22}$$

Among them, $\widetilde{\mathbf{F}}_i(B, t-\varepsilon) = P(X(t-\varepsilon) \ge B, \varphi(t-\varepsilon) = i)$ and $\mathbf{N}_{jk}(x_i, x_2; \varepsilon) = \partial \mathbf{F}_{jk}(x_1, x_2; \varepsilon)/\partial x_2$, in which $\mathbf{F}$ represents the expected number of crossings from (x_1, j) to (x_2, k) during a period ε. To maintain the stability of the whole system, we assume that the time t tends to infinity, and the probability of each state is as follows.

$$\mathbf{N}_{ij}(x,y) = \int_0^\infty \mathbf{N}_{ij}(x,y;t) dt \tag{23}$$

$$\lim_{t\to\infty} f_k(X(t), t) = \lim_{t\to\infty} A + \lim_{t\to\infty} B + \lim_{t\to\infty} C \tag{24}$$

We can have $\lim_{t\to\infty} \mathbf{N}_{ik}(P_{low}, X(t); t) = 0$ (Da Silva Soares and Latouche, 2006). Additionally, the abnormal death state follows from an energy level of either zero or P_{low}. Thus, we eventually obtain the steady density of the state (x, k) as follows.

$$\pi_k(x) = \sum_{i\in\boldsymbol{\Omega}_{EN}, j\in\boldsymbol{\Omega}_{EE}} \eta_N(0) \mathbf{R}_N(\mathbf{Q}_{NE})_{ij} \mathbf{N}_{jk}(0, x) + \sum_{i\in\boldsymbol{\Omega}_{EE}, j\in\boldsymbol{\Omega}_{EN}} \eta_E(B) \mathbf{R}_E(\mathbf{Q}_{EN})_{ij} \mathbf{N}_{jk}(B, x) \tag{25}$$

Therefore, the matrix expression of the steady state density is given by the following.

$$\pi(x) = (\eta_E(B), \eta_N(0)) \begin{bmatrix} \mathbf{R}_E & \mathbf{0} \\ \mathbf{0} & \mathbf{R}_N \end{bmatrix} \begin{bmatrix} \mathbf{0} & \mathbf{Q}_{EN} \\ \mathbf{Q}_{NE} & \mathbf{0} \end{bmatrix} \begin{bmatrix} \mathbf{N}_{jk}(0, x) \\ \mathbf{N}_{jk}(B, x) \end{bmatrix} \tag{26}$$

To solve the steady state probability density, we need to obtain $\eta_N(0), \eta_E(B), N_{jk}(0, x)$, and $N_{jk}(B, x)$. As stated above,

$N_{jk}(0,x)$ can be obtained by $N_E(0,x)$, and $N_{jk}(B,x)$ can be obtained by $N_N(B,x)$ when $x \neq 0$ and $x \neq B$. From (Ho et al., 2010), we obtain the following matrix equation.

$$\begin{bmatrix}\mathbf{N}_E(0,x)\\ \mathbf{N}_N(B,x)\end{bmatrix} = \begin{bmatrix} I & e^{KB}\psi \\ e^{K(B-x)}\hat{\psi} & I\end{bmatrix}^{-1} \begin{bmatrix} e^{Kx} & e^{Kx}\psi \\ e^{K(B-x)}\hat{\psi} & e^{K(B-x)}\end{bmatrix} \tag{27}$$

ψ records the first return probabilities to level x in a finite amount of time, which starting from fluid level $x, x \geq 0$, and it is known that ψ satisfies the Riccati equation (Bean et al., 2005).

$$\psi\mathbf{R}_N^{-1}\mathbf{Q}_{NE}\psi + \mathbf{R}_E^{-1}\mathbf{Q}_{EE}\psi + \psi\mathbf{R}_N^{-1}\mathbf{Q}_{NN} + \mathbf{R}_E^{-1}\mathbf{Q}_{EN} = 0 \tag{28}$$

Based on the definition of $N_{ij}(0,y)$, it is shown In Ho et al. (2010) the following.

$$\mathbf{N}_{ij}(0,x) = e^{Kx}\begin{bmatrix} I & \psi\end{bmatrix} \tag{29}$$

$$K = \mathbf{R}_E^{-1}\mathbf{Q}_{EE} + \psi\mathbf{R}_N^{-1}\mathbf{Q}_{NE} \tag{30}$$

$\hat{\psi}$ is the minimal nonnegative solution of the following Riccati equation, and it has a similar meaning to ψ.

$$\hat{\psi}\mathbf{R}_E^{-1}\mathbf{Q}_{EN}\hat{\psi} + \mathbf{R}_N^{-1}\mathbf{Q}_{NN}\hat{\psi} + \hat{\psi}\mathbf{R}_E^{-1}\mathbf{Q}_{EE} + \mathbf{R}_N^{-1}\mathbf{Q}_{NE} = 0 \tag{31}$$

Similarly, the corresponding $\hat{K}$ in (27) is as follows.

$$\hat{K} = \mathbf{R}_N^{-1}\mathbf{Q}_{NN} + \hat{\psi}\mathbf{R}_E^{-1}\mathbf{Q}_{EN} \tag{32}$$

Next, we calculate the boundary probability density masses $\eta_N(0)$ and $\eta_E(B)$. We define four first crossing probabilities with residual energy levels between zero and B.

- $(\chi_{EE})_{ij}$ refers to the probability of first reaching $(B,j), j \in \Omega_{EE}$, before returning to level zero, starting from $(0,i), i \in \Omega_{EE}$.
- $(\omega_{EN})_{ij}$ refers to the probability of first reaching $(0,j), j \in \Omega_{EN}$ before returning to level B, starting from $(0,i), i \in \Omega_{EE}$.
- $(\widetilde{\chi}_{EE})_{ij}$ refers to the probability of first reaching $(0,j), j \in \Omega_{EN}$ before returning to level B, starting from $(B,i), i \in \Omega_{EN}$.
- $(\widetilde{\omega}_{NE})_{ij}$ refers to the probability of first reaching $(B,j), j \in \Omega_{EE}$ before returning to level zero, starting from $(B,i), i \in \Omega_{EN}$.

Tang and Tan (2016) stated that the fluid queue model should satisfy the following boundary conditions.

$$\begin{cases}\eta_N(0)\left[\mathbf{T}_{DE}, \mathbf{T}_{DD}\right] - \boldsymbol{\pi}(0+)\mathbf{R}\begin{bmatrix}\boldsymbol{I} & \mathbf{0}\\ \mathbf{P}_{NE} & \mathbf{P}_{ND}\end{bmatrix} = \mathbf{0}\\ \boldsymbol{\pi}(B-)\mathbf{R} + \eta_E(B)\left[\mathbf{Q}_{EE}, \mathbf{Q}_{EN}\right] = \mathbf{0}\end{cases} \tag{33}$$

To determine $\boldsymbol{\pi}(0+)$ and $\boldsymbol{\pi}(B-)$, we consider using (26) and $\boldsymbol{\pi}(x) = (\boldsymbol{\pi}(x-), \boldsymbol{\pi}(x+))$. It is clear that $\mathbf{N}_E(0,0) = [I \;\; \omega_{EN}]$ and $\mathbf{N}_N(B,0) = [I \;\; \widetilde{\chi}_{NN}]$. Thus, we can obtain the equation as follows.

$$\boldsymbol{\pi}(0-) = \eta_N\mathbf{R}_N\mathbf{Q}_{NE}\boldsymbol{I} \tag{34}$$

$$\boldsymbol{\pi}(0+) = \eta_N(0)\mathbf{R}_N\mathbf{Q}_{NE}\omega_{EN} + \eta_E(B)\mathbf{R}_E\mathbf{Q}_{NE}\widetilde{\chi}_{NN} \tag{35}$$

Similarly, the following can be obtained.

$$\boldsymbol{\pi}(B-) = \eta_N(0)\mathbf{R}_N\mathbf{Q}_{NE}\chi_{EE} + \eta_E(B)\mathbf{R}_E\mathbf{Q}_{EN}\widetilde{\omega}_{EN} \tag{36}$$

By substituting the above equations (34), (35), and (36) into equation (33), we can obtain the boundary probability densities $\eta_N(0)$ and $\eta_E(B)$.

5 Performance analysis

After obtaining the steady node probability density, we now measure the performance of the model in this section, mainly measuring the abnormal death probability and the steady energy consumption of the nodes under different working modes.

The parameters for the numerical results using our model are set in Table 5. We model the rechargeable vehicle on the *Powercaster* transmitter (Powercast Corporation, http://www.powercastco.com/products/development-kits/), which radiates continuous RF waves at an energy level of $3W$ (Naderi et al., 2014).

Table 5 Parameter settings for the computational model

Parameter	*Value*	*Parameter*	*Value*
M	4	T_s	0.2 s
K	5	T_w	1.8 s
B	10 Joules	BI	0.3 s
d_S	1.8 mW	ATIM	0.02 s
d_L	88 mW	d_T	273 mW

5.1 Performance index

- *The probability of abnormal death*: We need to consider two causes of the abnormal death state. One is when the energy level is zero, and the other is when the energy level is less than P_{low}, both leading to the abnormal death of nodes. The symbol P_D is defined as the probability of abnormal death. To obtain the value of P_D, we need the boundary probability density $\eta_D(0)$ and the steady state density where the energy level is less than P_{low}. Thus, we obtain the expression of P_D as follows.

$$P_D = \eta_D(0) + \int_0^{P_{low}} \boldsymbol{\pi}(x)dx\mathbf{1} \tag{37}$$

- *Stationary energy consumption*: Based on the above statement, we know that nodes have different energy consumption rates under different conditions. It is meaningful to determine the steady state energy consumption per unit time because it can measure the overall performance of the node. Therefore, the stationary energy consumption E_{per} is calculated as follows.

$$E_{per} = \int_0^B \boldsymbol{\pi}(x)\mathbf{R}_d dx\mathbf{1} \tag{38}$$

5.2 Numerical results and analysis

We show some numerical results to illustrate the theoretical findings, which gives us a better understanding of the overall working state of nodes with abnormal death.

5.2.1 Impact of the number of sensor node

We investigate the effect of the number of sensor nodes on the abnormal death rate and stationary energy consumption under HSU and HTU. Figure 5 shows the effect of the sensor node density on the abnormal death rate, and Figure 6 represents the influence of the node density on stationary energy consumption. Considering changes in sensor node density, we set the data arrival rate as 50 frame/seconds, the vehicle moving rate as 2 meters/seconds, and the charging probability as 0.3. Figures 5(a) and 6(a) show the probability of abnormal death monotonically decreasing with an increasing number of sensor nodes. The reason is that, with an increased node density in the network, the competition among nodes increases, which leads to a decrease in the probability of transmitting a data frame in a randomly chosen time slot in the data window. The probability of abnormal death is positively correlated with the transmission probability. Meanwhile, as shown in Figures 5(b) and 6(b), stationary energy consumption corresponds with abnormal death probability, which is also due to the decreasing probability of transmitting a data frame in any chosen time slot. From another point of view, a decrease in stationary energy consumption directly reduces the probability of abnormal death. Thus, their trends should correspond with each other. Moreover, we can observe that the abnormal death probability increases as the maximum distance J between adjacent nodes increases in either mode. Correspondingly, the stationary energy consumption also increases. These ties in trends are because an increase in J results in the charging vehicle not reaching in time the node that needs charging, which increases the probability of abnormal death.

Comparing Figure 5(a) with Figure 6(a), it is shown that the minimum probability of abnormal death in HSU is approximately 0.249, while the maximum value in HTU is approximately 0.2415. The reason is that the net energy consumption needs to consider both the charging rate and the energy consumption in different states. In the long term, the charging process and working process will be parallel, which will reduce the overall energy consumption of the nodes and, thus, reduce the probability of abnormal death. In addition, corresponding to the change in the abnormal death rate, as shown in Figures 5(b) and 6(b), the stationary energy consumption of nodes in HTU is less than that those in HSU. Thus, the performance of HTU is better than that of HSU under the same conditions due to its lower node mortality and energy consumption.

Figure 5 Effect of the number of sensor nodes on abnormal death and stationary energy consumption in HSU: (a) effect of the number of sensor nodes on abnormal death in HSU and (b) effect of the number of sensor nodes on stationary energy consumption in HSU (see online version for colours)

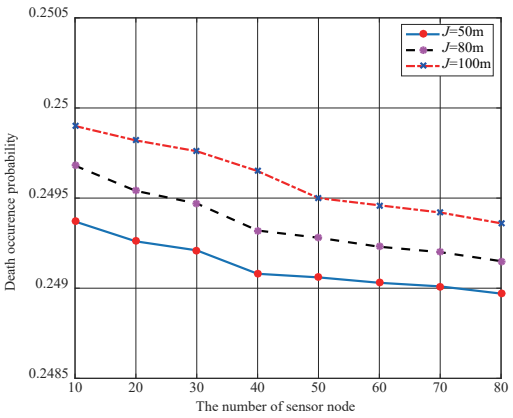

(a)

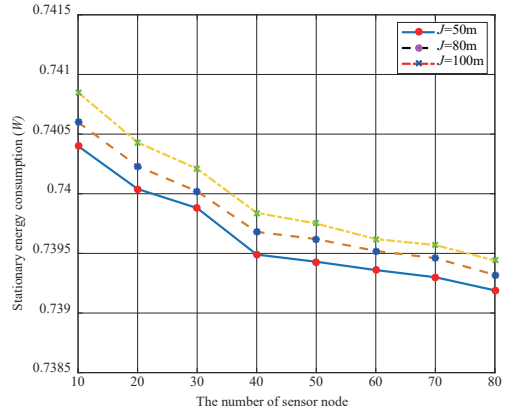

(b)

5.2.2 Impact of the data frame arrival rate

In Figures 7 and 8, we vary the rate of arrival of the data frames, and we show the change in the performance metrics, respectively. We observe the performance variety by changing the data frame arrival rate and set the number of sensor nodes as 10 in the network and the distance J as 50 meters and maintain the charging probability as 0.3. It is shown in Figures 7(a) and Figure 8(a) that the rate of node mortality increases with an increased rate of arrival of data frames because it indicates that the amount of communication is increased; thus, the energy consumed is also increased, which may result a failure of the wireless charging vehicle to arrive at the nodes needing to be charged in time. Meanwhile, shown in Figures 7(b) and Figure 8(b), the stationary energy consumption also increases with an increased arrival rate, which can be interpreted as the network load increases that result in the stationary energy consumed increasing in a duty cycling. Furthermore, when the

data frame arrival rate is 60 frames/second, the load reaches saturation, and the abnormal death rate tends to be stable. We can also observe that the abnormal death occurrence probability and the stationary energy consumption decrease as the moving rate of the vehicle increases. This can be interpreted as the node being charged as soon as possible, which would reduce the abnormal death probability due to insufficient energy.

Figure 6 Effect of the number of sensor nodes on abnormal death and stationary energy consumption in HTU: (a) effect of the number of sensor nodes on abnormal death in HTU and (b) effect of the number of sensor nodes on stationary energy consumption in HTU (see online version for colours)

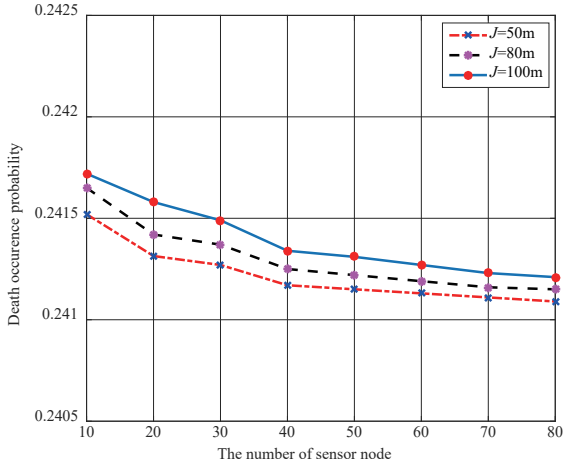

(a)

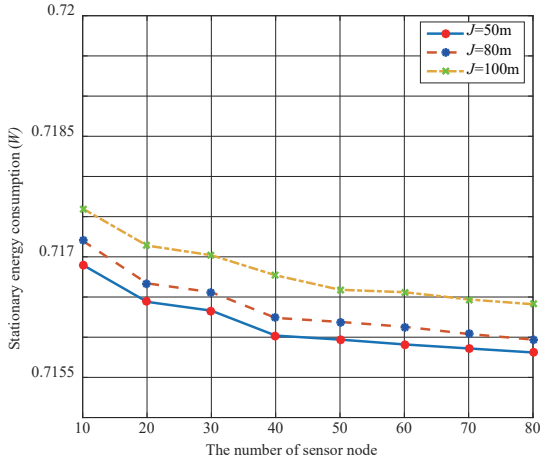

(b)

We observe the comparison of two performance metrics with different data frame arrival rates in Figures 7 and 8. We can see that the probability density has the same tendencies in the two modes; however, the range of change is greater in HTU because, once the energy buffer reaches P_{low} under the charging state, the node will immediately work as normal. The charging process proceeds in parallel with the working process until the energy buffer is full and the vehicle leaves. In parallel work, the increasing load leads to a relatively obvious change in energy. Correspondingly, the abnormal death rate has the same change. Similarly, as shown in Figures 7(b) and 8(b), the range of the stationary energy consumption in HTU is larger than HSU because an excessive load results in a significant energy change. However, we can also observe that the value of the abnormal death or the stationary energy consumption in HTU is always lower than that in HSU. Thus, we can say that, in terms of the abnormal death rate and the stationary energy consumption, the performance of a node working in HTU is better than a node working in HSU when the number of nodes and the charging probability remain unchanged.

Figure 7 Effect of the data frame arrival rate on abnormal and stationary energy consumption in HSU: (a) effect of the data frame arrival rate on abnormal death in HSU and (b) effect of the data frame arrival rate on stationary energy consumption in HSU (see online version for colours)

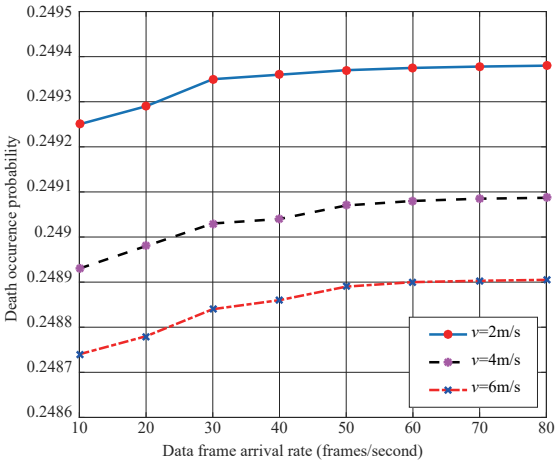

(a)

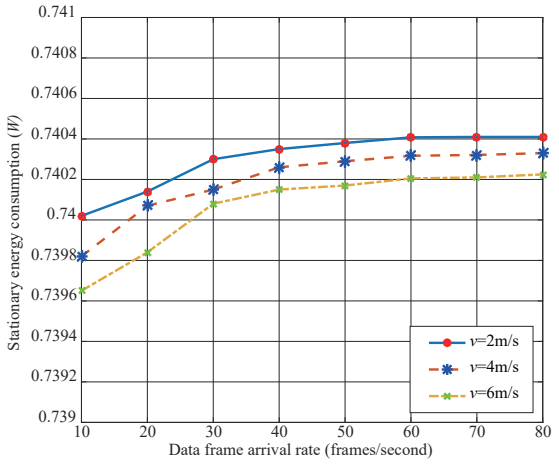

(b)

5.2.3 *Impact of the charging probability*

In this subsection, we investigate the influence of charging probability on the abnormal death rate and energy consumption. Considering the node working in HSU, Figure 9(a) shows the abnormal death rate under different charging probability and sensor node density in network. As expected, the death occurrence probability decreases with charging probability increasing. This can be explained that when the node needs recharging, the probability that the node can replenish the power immediately increases. The residual energy is relatively sufficient to support the energy

consumption that reduces the probability of the abnormal death.

Figure 9(b) shows the comparison of the stationary energy consumption under different charging probability. It is shown that the stationary energy consumption significantly reduces with an increased charging probability. The reason for this phenomenon is that the charging rate of the node is much larger than the power consumption rate of each state. Thus, the energy accumulation is greater than the energy consumption in duty cycling in the long run. This observation indicates that, in the optimisation of network performance, the probability of charging should be increased to reduce the stationary energy consumption and the probability of node abnormal death.

In short, although we only show the effect of the charging probability in HSU, the same conclusion applies to nodes operating in HTU. Increasing the probability of charging can reduce the abnormal death probability, which is very important to improve the overall performance of the network. Therefore, it is essential to ensure the optimal charging probability of the charging vehicle in the network and to ensure the continuous operation of the network.

Figure 8 Effect of the data frame arrival rate on abnormal and stationary energy consumption in HTU: (a) effect of the data frame arrival rate on abnormal death in HTU and effect of the data frame arrival rate on stationary energy consumption in HTU (see online version for colours)

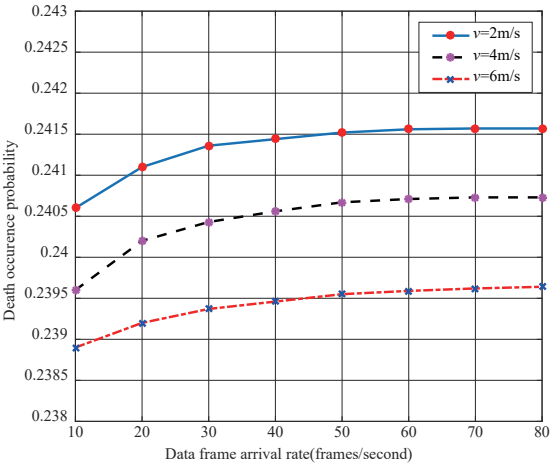

(a)

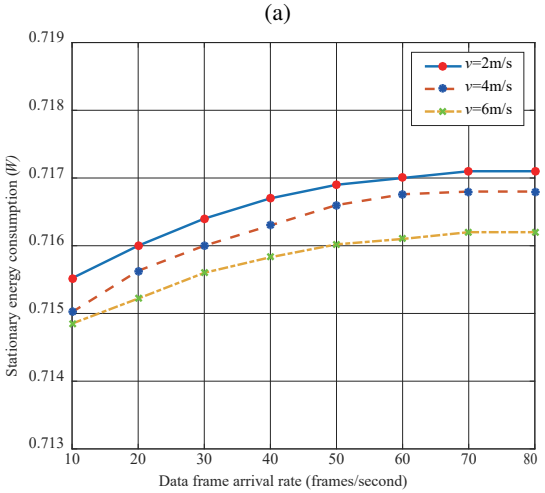

(b)

Figure 9 Effect of the charging probability on abnormal death and stationary energy consumption in HSU: (a) effect of the charging probability on abnormal death in HSU and (b) effect of the charging probability on stationary energy consumption in HSU (see online version for colours)

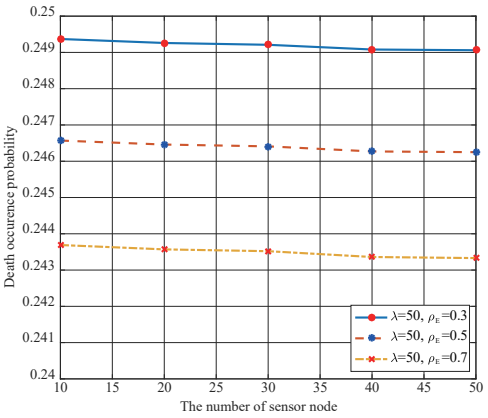

(a)

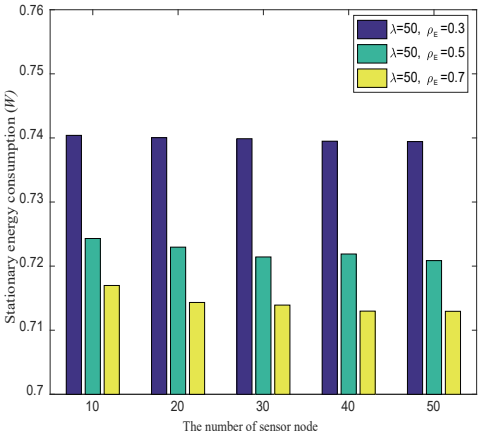

(b)

Table 6 Parameter values for simulation

Parameter	*Value*	*Parameter*	*Value*
PHY header	192 bits	MAC header	224 bits
ACK	112 bits	Packet payload	8192 bits
CW_{min}	31	CW_{max}	1023
Propagation delay	1 μs	Slot time	20 μs
SIFS	10 μs	DIFS	50 μs

5.2.4 *Comparison with simulation*

To verify the accuracy of the model, the numerical results of MATLAB and the simulation results of the network simulator NS-3 are compared in this paper. To make the simulation model and scene setting uniform, we modify the NS-3 simulation platform with the random selection of backoff value function and the propagation delay function. The node adopts the basic access method, and the physical layer nodes use DSSS debugging mechanism; the simulation parameters are shown in Table 6. In the numerical experiment, the specific probabilities, obtained under different parameters according to the model In Swain et al. (2014) and Table 2, are listed

Table 7 State transition probabilities

From	*to*	λ=10	λ=20	λ=30	λ=40	λ=50	λ=60	λ=70	λ=80
S	L	0.5815	0.5815	0.5815	0.5815	0.5815	0.5815	0.5815	0.5815
L	$A(1,1)$	0.0013	0.0158	0.0228	0.0264	0.0286	0.0298	0.0313	0.0321
$A(K,M)$	S	1	1	1	1	1	1	1	1
$A(i,j)$	$A(i,j+1)$	0.012	0.1338	0.1871	0.2139	0.2302	0.245	0.2489	0.2548
$A(i,j)$	$A(i+1,1)$	0.0013	0.0137	0.0185	0.0208	0.022	0.0225	0.0235	0.0239
$A(m,M)$	$A(m+1,1)$	0.0013	0.0158	0.0228	0.0264	0.0286	0.0298	0.0313	0.0321
$A(K,j)$	S	0.988	0.8662	0.8129	0.7861	0.7698	0.755	0.7511	0.7452

in Table 7, and the contrast result is shown in Figure 10. We consider 100 nodes randomly distributed in 300×300 m network region. The charging vehicle starts from a random selected node; then, it periodically travels all nodes in the scene and returns to the starting node. When the energy of the node reaches P_{low} (0.605×10^{-2}Joules), the node will return to normal work (in HTU). We can see that our model is in agreement with the simulation. The abnormal death probability calculated by the model is approximately 0.1% different from the probability of death obtained by the simulation. This result shows that the model proposed in this paper can accurately predict the probability of abnormal death.

Figure 10 The comparison result under different data frame arrival rates (see online version for colours)

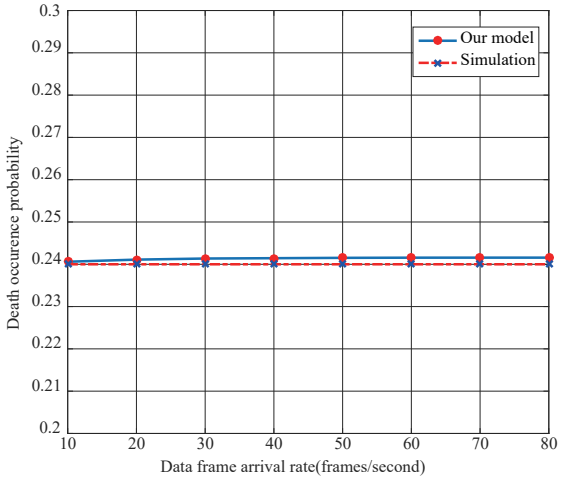

6 Conclusion

WET-based WRSNs can effectively alleviate the node energy problem in WSNs and provide relatively stable energy compared with EH-based WRSNs. However, the nodes may fall into a state of abnormal death due to the sudden increase in data traffic, which should not be neglected in future practical applications. In this paper, we use a multilayer MFQ model to evaluate sensor nodes in WRSNs with the state of abnormal death. We also compared the performance of the node with abnormal death for two charging modes. In HSU, the charging process and the working process of the node are performed in series. In HTU, the charging process is in parallel with the node's working process. We analyse the performance using this model by calculating the abnormal death probability and steady energy consumption. We mainly focus on the impact of different parameter settings on the two performance metrics. Through the numerical results shown in this paper, it can be clearly observed that the abnormal death and stationary energy consumption have basically the same change trends regardless of the parameters. To reduce the probability of abnormal death, we can adjust the suitable parameters to reduce the overall energy consumption in the network, i.e., select the optimum data frame arrival rate, which controls the network load. Meanwhile, by comparing the two energy usage modes, we find that HTU is better than HSU. Therefore, HTU can reduce the abnormal death node in practical applications. In brief, the model proposed in this paper can be applied to network optimisation and practical application design.

Acknowledgement

The work described in this paper was supported by the grant from the National Natural Science Foundation of China (No. 61502540, No. 61402542), the National Science Foundation of Hunan Province (No. 2019JJ40406, No. 2018JJ3692), the Innovation Training Grant for Students of Central South University (No. GCX2020347Y), and the Fundamental Research Funds for the Central Universities of Central South University (China) under Grant (No. 2020zzts592).

References

Bean, N.G., O'Reilly, M.M. and Taylor, P.G. (2005) 'Hitting probabilities and hitting times for stochastic fluid flows', *Stochastic processes and their applications*, Vol. 115, No. 9, pp.1530–1556.

Biason, A. and Zorzi, M. (2015) 'Transmission policies for an energy harvesting device with a data queue', *2015 International Conference on Computing, Networking and Communications (ICNC)*, Garden Grove, CA, USA, pp.189–195.

Biason, A., Del, T.D. and Zorzi, M. (2014) 'Low-complexity policies for wireless sensor networks with two energy harvesting devices', *2014 13th Annual Mediterranean Ad Hoc Networking Workshop (MED-HOC-NET)*, Piran, Slovenia, pp.180–187.

Chan, .W.H.R., Zhang, P., Nevat, I., Nagarajan, S G., Valera, A C., Tan, H-X. and Gautam, N. (2015) 'Adaptive duty cycling in sensor networks with energy harvesting using continuous-time Markov chain and fluid models', *IEEE Journal on Selected Areas in Communications*, Vol. 33, No. 12, pp.2687–2700.

Correia, R., Boaventura, A. and Carvalho, N. B. (2017) 'Quadrature amplitude backscatter modulator for passive wireless sensors in IoT applications', *IEEE Transactions on Microwave Theory and Techniques*, Vol. 65, No. 4, pp.1103–1110.

Da Silva Soares, A. and Latouche, G. (2009) 'Fluid queues with level dependent evolution', *European Journal of Operational Research*, Vol. 196, No. 3, pp.1041–1048.

Da Silva Soares, A. and Latouche, G. (2006) 'Matrix-analytic methods for fluid queues with finite buffers', *Performance Evaluation*, Vol. 63, No. 4-5, pp.295–314.

Deng, R., Zhang, Y., He, S., Chen, J. and Shen, X. (2016) 'Maximizing network utility of rechargeable sensor networks with spatiotemporally coupled constraints', *IEEE Journal on Selected Areas in Communications*, Vol. 34, No. 5, pp.1307–1319.

Gao, J., Wang, J., Zhong, P. and Wang, H. (2017) 'On threshold-free error detection for industrial wireless sensor networks', *IEEE Transactions on Industrial Informatics*, Vol. 14, No. 5, pp.2199–2209.

Guimarães, D.A., Frigieri, E P. and Sakai, L J. (2020) 'Influence of node mobility, recharge, and path loss on the optimized lifetime of wireless rechargeable sensor networks', *Ad Hoc Networks*, Vol. 97, pp.102025.

Ho, C.K., Khoa, P.D. and Ming, P.C. (2010) 'Markovian models for harvested energy in wireless communications', *2010 IEEE International Conference on Communication Systems*, Singapore, pp.311–315.

Jan, B., Farman, H., Javed, H., Montrucchio, B., Khan, M. and Ali, S. (2017) 'Energy efficient hierarchical clustering approaches in wireless sensor networks: A survey', *Wireless Communications and Mobile Computing*, Vol. 2017.

Jung, D., Teixeira, T. and Savvides, A. (2009) 'Sensor node lifetime analysis: Models and tools', *ACM Transactions on Sensor Networks (TOSN)*, Vol. 5, No. 1, pp.1–33.

Kaur, P., Sohi, B.S. and Singh, P. (2019) 'Recent advances in MAC protocols for the energy harvesting based WSN: A comprehensive review', *Wireless Personal Communications*, Vol. 104, No. 1, pp.423–440.

Lei, J., Yates, R. and Greenstein, L. (2009) 'A generic model for optimizing single-hop transmission policy of replenishable sensors', *IEEE Transactions on Wireless Communications*, Vol. 8, No. 2, pp.547–551.

Lin, C., Wang, Z., Han, D., Wu, Y., Yu, C W.and Wu, G. (2016) 'TADP: Enabling temporal and distantial priority scheduling for on-demand charging architecture in wireless rechargeable sensor networks', *Journal of Systems Architecture*, Vol. 70, pp.26–38.

Liu, X., Dong, M., Liu, Y., Liu, A. and Xiong, N.N (2018) 'Construction low complexity and low delay CDS for big data code dissemination', *Complexity*, Vol. 2018.

Liu, A., Huang, M., Zhao, M. and Wang, T. (2018) 'A smart high-speed backbone path construction approach for energy and delay optimization in WSNs', *IEEE Access*, Vol. 6, pp.13836–13854.

Lu, X., Wang, P., Niyato, D., Kim, D I. and Han, Z. (2015) 'Wireless charging technologies: Fundamentals, standards, and network applications', *IEEE Communications Surveys & Tutorials*, Vol. 18, No. 2, pp.1413–1452.

Masotti, D., Costanzo, A., Del Prete, M. and Rizzoli, V. (2016) 'Time-modulation of linear arrays for real-time reconfigurable wireless power transmission', *IEEE Transactions on Microwave Theory and Techniques*, Vol. 64, No. 2, pp.331–342.

Mukherjee, M., Shu, L., Hu, L., Hancke, G P. and Zhu, C.(2017) 'Sleep scheduling in industrial wireless sensor networks for toxic gas monitoring', *IEEE Wireless Communications*, Vol. 24, No. 4, pp.106–112.

Naderi, M.Y. and Basagni, S. and Chowdhury, K.R. (2012) 'Modeling the residual energy and lifetime of energy harvesting sensor nodes', *2012 IEEE Global Communications Conference (GLOBECOM)*, Anaheim, CA, USA, pp.3394–3400.

Naderi, M.Y., Nintanavongsa, P. and Chowdhury, K.R. (2014) 'RF-MAC: A medium access control protocol for re-chargeable sensor networks powered by wireless energy harvesting', *IEEE Transactions on Wireless Communications*, Vol. 13, No. 7, pp.3926–937.

Naderi, M.Y., Chowdhury, K.R and Basagni, S. (2015) 'Wireless sensor networks with RF energy harvesting: Energy models and analysis', *2015 IEEE Wireless Communications and Networking Conference (WCNC)*, New Orleans, LA, USA, pp.1494–1499.

Powercast Corporation, Lifetime Power Evaluation and Development Ki [Online]. Available: http://www.powercastco.com/products/development-kits/.

Ryu, H., Yoon, H-J. and Kim, S-W. (2019) 'Hybrid energy harvesters: toward sustainable energy harvesting', *Advanced Materials*, Vol. 31, No. 34, pp.1802898.

Sah, D K. and Amgoth, T. (2020) 'Renewable energy harvesting schemes in wireless sensor networks: a Survey', *Information Fusion*, Vol. 63, pp.223–247.

Sah, D. Kumar and Amgoth, T. (2020) 'A novel efficient clustering protocol for energy harvesting in wireless sensor networks', *WIRELESS NETWORKS*.

Seyedi, A. and Sikdar, B. (2008) 'Modeling and analysis of energy harvesting nodes in wireless sensor networks', *2008 46th Annual Allerton Conference on Communication, Control, and Computing*, Monticello, IL, USA, pp.67–71.

Shu, Y., Shin, K G., Chen, J. and Sun, Y. (2016) 'Joint energy replenishment and operation scheduling in wireless rechargeable sensor networks', *IEEE Transactions on Industrial Informatics*, Vol. 13, No. 1, pp.125–134.

Singh, J., Kaur, R. and Singh, D. (2020) 'A Survey and Taxonomy on Energy Management Schemes in Wireless Sensor Networks', *AJournal of Systems Architecture*, pp.101782.

Sudevalayam, S., Kulkarni, P. (2010) 'Energy harvesting sensor nodes: Survey and implications', *IEEE Communications Surveys & Tutorials*, Vol. 13, No. 3, pp.443–461.

Susu, A.E., Acquaviva, A., Atienza, D. and De Micheli, G. (2008) 'Stochastic modeling and analysis for environmentally powered wireless sensor nodes', *2008 6th International Symposium on Modeling and Optimization in Mobile, Ad Hoc, and Wireless Networks and Workshops*, Berlin, Germany, pp.125–134.

Swain, P., Chakraborty, S., Nandi, S. and Bhaduri, P. (2014) 'Performance modeling and analysis of IEEE 802.11 IBSS PSM in different traffic conditions', *IEEE Transactions on Mobile Computing*, Vol. 14, No. 8, pp.1644–1658.

Tan, L. and Tang, S. (2016) 'Energy harvesting wireless sensor node with temporal death: Novel models and analyses', *IEEE/ACM Transactions on Networking*, Vol. 25, No. 2, pp.896–909.

Tang, S. and Tan, L. (2016) 'Reward rate maximization and optimal transmission policy of EH device with temporal death in EH-WSNs', *IEEE Transactions on Wireless Communications*, Vol. 16, No. 2, pp.1157–1167.

Tang, J., Liu, A., Zhang, J., Xiong, N N., Zeng, Z. and Wang, T. (2018) 'A trust-based secure routing scheme using the traceback approach for energy-harvesting wireless sensor networks', *Sensors*, Vol. 18, No. 3, pp.751.

Tomar, A., Muduli, L. and Jana, P K. (2016) 'An efficient scheduling scheme for on-demand mobile charging in wireless rechargeable sensor networks', *Pervasive and Mobile Computing*, Vol. 59, pp.101074.

Tunc, C. and Akar, N. (2017) 'Markov fluid queue model of an energy harvesting IoT device with adaptive sensing', *Performance Evaluation*, Vol. 111, pp.1–16.

Ventura, J. and Chowdhury, K. (2011) 'Markov modeling of energy harvesting body sensor networks', *2011 IEEE 22nd International Symposium on Personal, Indoor and Mobile Radio Communications*, Toronto, ON, Canada, pp.2168–2172.

Wu, Q., Sun, P. and Boukerche, A. (2020) 'A novel joint data gathering and wireless charging scheme for sustainable wireless sensor networks', *ICC 2020–2020 IEEE International Conference on Communications (ICC)*, Dublin, Ireland, pp.1–6.

Zhang, H., Guo, Y-x., Zhong, Z. and Wu, W. (2019) 'Cooperative integration of RF energy harvesting and dedicated WPT for wireless sensor networks', *IEEE Microwave and Wireless Components Letters*, Vol. 29, No. 4, pp.291–293.

Zhang, S. (2013) *Modeling, Analysis and Design of Energy Harvesting Communication Systems*, Ph.D. dissertation, Dept. Elect. Comput. Eng., Univ. Rochester, NY, USA.

Zheng, R., Hou, J. and Sha, L. (2004) 'Performance analysis of the IEEE 802.11 power saving mode', *Proc. CNDS*.

Zhong, P., Zhang, Y., Ma, S., Kui, X. and Gao, J. (2018) 'RCSS: A real-time on-demand charging scheduling scheme for wireless rechargeable sensor networks', *Sensors*, Vol. 18, No. 5, pp.1–18.

Zhou, P., Wang, C. and Yang, Y. (2019) 'Self-sustainable sensor networks with multi-source energy harvesting and wireless charging', *IEEE INFOCOM 2019-IEEE Conference on Computer Communications*, Paris, France, pp.1828–1836.

Supplemental material

Table S1 lists the major notations used throughout the paper.

Table S1 Summary of notation

Notation	*Definition*
X	The residual energy change of sensors, $X = \{X(t), 0 \leq X(t) \leq B, t \geq 0\}$
B	Energy buffer size
P_{low}	The lower charging threshold
P_{high}	The upper charging threshold

Table S1 Summary of notation (continued)

Notation	*Definition*
P_{SD}	The probability of the node switches to D from S
P_{SE}	The probability of charging in S
P_{SL}	The probability of the node switches to L from S
P_{LS}	The probability of the node switches to S from L
P_{LD}	The probability of the node switches to D from L
P_{LE}	The probability of charging in L
T_S	A fixed sleeping period
T_w	The wakeup stage
J	The farthest distance between contiguous nodes
d_S	The energy consumption rate in the state S
v	The moving speed of the vehicle
τ	The probability of sending a data frame
M	The maximum retransmission time
T_{tr}	The exponential distribution of mean
$\{A\}$	The transmission process of the nodes, $\{A\} = \{A(k,m)\}$,$\{1 \leq k \leq K, 1 \leq m \leq M\}$
k	The data frame in the data buffer pool
m	The number of retransmissions
φ_T	The working process of the node
φ_E	The charging process of the node
φ	The process combine φ_T with φ_E
$\mathbf{\Omega}_T$	The state space of working process
$\mathbf{\Omega}_E$	The state space of charing process
$\mathbf{\Omega}$	The state space of φ
$\mathbf{\Omega}_{EE}$	The charging state space
$\mathbf{\Omega}_{EN}$	The noncharging state space
$\mathbf{Q}_T$	The infinitesimal generator of $\mathbf{\Omega}_T$
$\mathbf{Q}_E$	The infinitesimal generator of φ_E
$\mathbf{Q}$	The infinitesimal generator of φ
$d_{\varphi_T(t)}$	The energy consumption rate at time t
d_E	The energy consumption rate in the state E
d_S	The energy consumption rate in S
d_T	The energy consumption rate in the state T
d_L	The energy consumption rate in the state L
r_i	The net charge rate
μ	The mean drift of the fluid queue model that exists
ψ	The minimal nonnegative solution
K	The maximum number of frames
$\boldsymbol{\xi}$	The steady state probability vector
ψ	The first return probabilities to level x in a finite amount of time
ε	The constant that tends to 0_+
$\boldsymbol{\pi}(x)$	The steady state density vector
ρ_E	The conversion probability from E to N
ρ_N	The conversion probability from N to E
P_D	The probability of abnormal death.
$\eta_D(0)$	The boundary probability density
E_{pre}	The stationary energy consumption